

# Accuracy of the ADNEX MR scoring system based on a simplified MRI protocol for the assessment of adnexal masses

Patrick N. Pereira 

Luis O. Sarian 

Adriana Yoshida 

Karla G. Araújo 

Ricardo H. O. Barros 

Ana C. Baião

Daniella B. Parente 

Sophie Derchain 

## PURPOSE

We aimed to evaluate the ADNEX MR scoring system for the prediction of adnexal mass malignancy, using a simplified magnetic resonance imaging (MRI) protocol.

## METHODS

In this prospective study, 200 patients with 237 adnexal masses underwent MRI between February 2014 and February 2016 and were followed until February 2017. Two radiologists calculated ADNEX MR scores using an MRI protocol with a simplified dynamic study, not a high temporal resolution study, as originally proposed. Sensitivity, specificity, positive and negative predictive values, likelihood ratios, and the area under the receiver operating characteristic curve were calculated (cutoff for malignancy, score  $\geq 4$ ). The reference standard was histopathologic diagnosis or imaging findings during  $>12$  months of follow-up.

## RESULTS

Of 237 lesions, 79 (33.3%) were malignant. The ADNEX MR scoring system, using a simplified MRI protocol, showed 94.9% (95% confidence interval [CI], 87.5%–98.6%) sensitivity and 97.5% (95% CI, 93.6%–99.3%) specificity in malignancy prediction; it was thus highly accurate, like the original system. The level of interobserver agreement on simplified scoring was high ( $\kappa = 0.91$ ).

## CONCLUSION

In a tertiary cancer center, the ADNEX MR scoring system, even based on a simplified MRI protocol, performed well in the prediction of malignant adnexal masses. This scoring system may enable the standardization of MRI reporting on adnexal masses, thereby improving communication between radiologists and gynecologists.

From the Department of Obstetrics and Gynecology (P.N.P. ✉ [patricknunes@gmail.com](mailto:patricknunes@gmail.com), L.O.S., A.Y., K.G.A., A.C.B., S.D.) State University of Campinas-Unicamp, Campinas Faculty of Medical Sciences, São Paulo, Brazil; Section of Imaginology (P.N.P., R.H.O.B.), Sumaré State Hospital, Sumaré, São Paulo, Brazil; Department of Radiology (D.B.P.), Federal University of Rio de Janeiro National Faculty of Medicine, Rio de Janeiro, RJ, Brazil.

Received 20 September 2017; revision requested 30 October 2017; last revision received 8 January 2018; accepted 12 January 2018.

Published online 16 February 2018.

DOI 10.5152/dir.2018.17378

Adnexal masses are frequent findings in pelvic and abdominal imaging studies, such as those conducted with ultrasonography (US), computed tomography (CT), and magnetic resonance imaging (MRI) (1). Preoperative evaluation of these lesions and determination of the risk of malignancy are critical to define treatment. A lesion with a low risk of malignancy can be followed or treated with minimally invasive surgery performed by a general gynecologist. When the risk of malignancy is significant, the patient should be referred to a tertiary center for treatment by a multidisciplinary team that includes an oncologic gynecologist (2, 3).

Every year, about 240 000 women worldwide are diagnosed with ovarian cancer. The 5-year survival rate is less than 45%, and ovarian cancer is responsible for about 150 000 deaths annually. Thus, it is the seventh most common cancer and the eighth most common cause of cancer death among women (4).

US is the first-line modality for the assessment of suspected adnexal masses, with very accurate results (5). However, US examination yields indeterminate findings in approximately 20% of adnexal masses (6–8). Exophytic and large tumors, fatty components, clots that mimic vegetation, and fibrous tumors have morphologic characteristics that are difficult to interpret with US. Other imaging methods (e.g., MRI, CT, positron emission tomography–computed tomography [PET-CT]) are under investigation as stand-alone examinations or for use in combination with US in the evaluation of these masses (9–12). MRI has

You may cite this article as: Pereira PN, Sarian LO, Yoshida A, et al. Accuracy of the ADNEX MR scoring system based on a simplified MRI protocol for the assessment of adnexal masses. *Diagn Interv Radiol* 2018; 24:63–71.

the best potential for preoperative evaluation of adnexal masses. It has shown greater accuracy (88.9%) than transvaginal US (63.9%) in the characterization of adnexal masses as malignant, and better specificity (83.7% vs. 39.5%) (13). Systematic reviews showed that MRI has improved the preoperative evaluation of suspicious adnexal lesions. In the evaluation of ultrasound-in-determinate adnexal lesions, MRI could be considered as the gold standard, highlighting the high specificity of this imaging method in the characterization of benign lesions (13, 14).

Various MRI protocols have been used to evaluate ovarian lesions, and MRI reporting methods vary among institutions (15, 16). In an attempt to standardize imaging evaluation and reporting and to facilitate communication between gynecologists and radiologists, Thomassin-Naggara et al. (17) published the MRI scoring system for adnexal lesions (ADNEX MR scoring system) in 2013. This protocol has a structure similar to that of the Breast Imaging Report Data System (BI-RADS™), with a sensitivity of 93.5% and specificity of 96.6% in the detection of malignant adnexal masses (17). However, one of the main parts of the protocol is the acquisition and post-processing of perfusion-weighted magnetic resonance images obtained by using a dynamic contrast-enhanced T1-weighted gradient-echo sequence. This sequence is technically demanding, and the required temporal resolution for the originally proposed dynamic contrast-enhanced study is 2.4 s. Another great limitation is the lack of widespread use of perfusion MRI in current clinical practice, in some regions, recognized even by scoring authors (18). Also, some post-processing techniques can be complex, such as the semiquantitative analysis based on relative signal intensity of the curve, used to calculate the initial area under the curve

(before 60 s) and different mathematic models used to obtain the enhancement amplitude, time of half rising, and maximal slope of the curve.

The objective of this study was to test the ADNEX MR scoring system, based on a simplified MRI protocol, using a simple dynamic study with high spatial resolution at 30, 60, 90, 120, and 150 s acquisitions. We believe that this scoring approach is promising for the standardization of MRI evaluation and reporting, which is urgently needed to improve team communication and has been performed successfully for other organs, such as the breast (BI-RADS™), prostate (Prostate Imaging Reporting and Data System; PI-RADS™), and liver (Liver Imaging Reporting and Data System; LI-RADS™). We used histopathologic and long-term clinical follow-up data as the standard reference. To our knowledge, this study is the first to evaluate the ADNEX MR scoring system using a simplified MRI protocol, besides having the highest number of adnexal masses evaluated.

## Methods

### Patients

This prospective study was conducted at the Faculty of Medical Sciences of the State University of Campinas. All medical procedures and examinations were performed at the Women's Prof. José Aristodemo Pinotti Women's Hospital and Sumaré State Hospital, which are medical facilities that compose the healthcare area of Unicamp. The Women's Hospital, also known as Caism, is a hospital with a gynecologic oncology reference unit of regional and national scope. Written informed consent was obtained from all patients. The study was approved by the university's Research Ethics Committee (protocol nos. 1092/2009 and 008/2010).

Two hundred women who had been referred to the oncology clinic of Women's Hospital due to the detection of adnexal masses between February 2014 and February 2016 were prospectively invited to participate. We randomly invited women referred to our hospital because of an adnexal mass, with the recruiter not knowing

### Main points

- ADNEX MR scoring system, based on a simplified MRI protocol, is a useful tool in the assessment of adnexal masses.
- This system helps the standardization of MRI reports for adnexal masses.
- Very high interobserver agreement was obtained using the simplified protocol.
- Borderline tumors remain a diagnostic challenge.

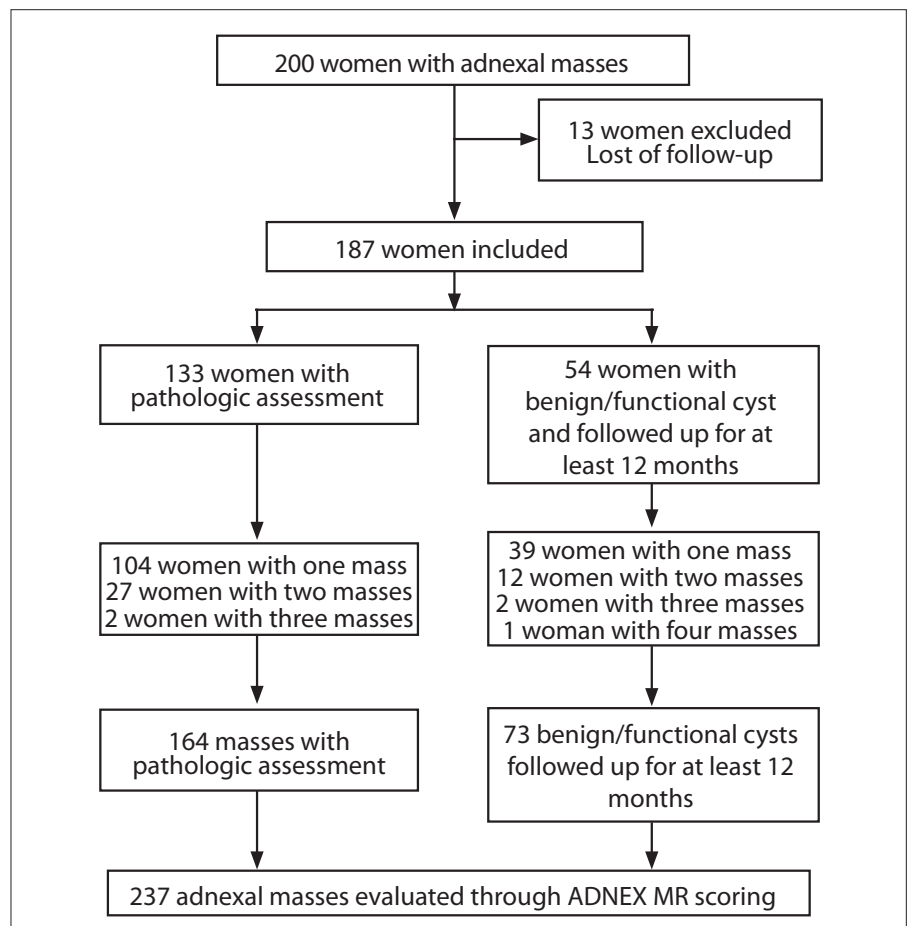


Figure 1. Flow-chart depiction of patient selection.

clinical information (time of evolution, for example), laboratory tests (serum levels of CA-125) or imaging of the patient (pelvic US), trying to avoid any selection biases.

MRI examinations were performed after thorough pelvic examination. We included all women with adnexal masses for whom histologic results were available or who had been followed for at least 1 year (until February 2017), as proposed by Thomassin-Naggara et al. (17). We also included women discharged from our oncology facility due to benign clinical findings, such as functional cysts, endometrioma or hydrosalpinx, and those whose adnexal masses had disappeared on follow-up examinations.

Fig. 1 illustrates patient allocation. In total, 200 women were evaluated using ADNEX MR scoring system based on simplified MRI protocol. Of these, 13 women were excluded because they had no medical indication for surgery or did not complete 12 months of follow-up after diagnosis of the adnexal masses. The adnexal masses were excised via laparoscopy or laparotomy for histopathologic assessment. For the 13 unresectable tumors encountered, pathologic specimens were obtained by percutaneous biopsy of the pelvic masses or from abdominal implants. In total, 164 adnexal masses (from 104 women with single masses, 27 women with two masses each, and 2 women with three masses each) were evaluated histologically.

Of 54 women with no surgical indication due to benign/functional characteristics of the adnexal masses, 39 women had single masses, 12 women had bilateral masses, 2 women had three masses each, and 1 woman had four masses (total, 73 masses). None of these women showed worsening on follow-up imaging studies for at least 12 months.

### MRI protocol and evaluation

Patients fasted for 3 hours before undergoing MRI performed with a 1.5 Tesla device (GE Signa HDxt<sup>®</sup>; General Electric) using an 8-channel pelvic phased-array coil. Table 1 details the technical parameters of the MRI sequences used. Axial, sagittal, and coronal T2-weighted fast spin-echo sequences, axial T2-weighted sequences with fat suppression, and T1-weighted sequences with and without fat suppression were performed. Diffusion-weighted images were acquired in the axial plane, with b values of 0, 500, and 1000 s/mm<sup>2</sup>, as we routinely used in clinical practice. We used three-dimension-

al pre- and post-contrast (LAVA<sup>®</sup>) (TE, 2.1; TR, 4.3; FA, 12; slice thickness, 3.8 mm; inter-section gap, 2.0 mm; FOV, 320×192). After intravenous gadolinium injection, the dynamic study was performed in 5 post-contrast phases with 30 s delay each. Gadolinium chelate (Omniscan, 0.2 mL/kg body weight; GE Healthcare<sup>®</sup>) was administered at a rate of 3.5 mL/s using a power injector (Medrad), followed by a 10 mL infusion of normal saline. In the postprocessing of images, regions of interest (ROI) were selected and qualitative criteria were performed for diffusion-weighted restriction, as proposed by Thomassin-Naggara et al. (17), avoiding areas of necrosis. The postprocessing of the dynamic study included the absolute signal and the relative enhancement to build the dynamic curves.

Two radiologists (P.N.P. with 7 years of experience in body MRI, with an emphasis on gynecological pathologies and R.H.O.B. with 6 years of experience in body MRI, with an emphasis in gastrointestinal pathologies) independently evaluated MRI data from all patients and calculated ADNEX MR scores for all 237 adnexal masses. Interobserver agreement on these scores was evaluated. This was a prospective double-blind study, as the evaluators had no knowledge of the US reports, histologic and/or follow-up results.

ADNEX MR scores are based only on MRI parameters, as follows (17):

1. No adnexal mass;
2. Benign mass: purely cystic, with the presence of endometrioid or fatty masses; or absence of wall enhancement in masses without solid tissue; or low signal on diffusion- or T2-weighted images within solid tissue; or masses with solid tissue with curve type 2 or nonfeasible and absence of wall enhancement.
3. Probably benign mass: wall enhancement in masses without solid tissue or type 1 time-signal intensity curve within solid tissue;
4. Indeterminate mass: type 2 time-signal intensity curve within solid tissue and wall enhancement;
5. Probably malignant mass: peritoneal implants or type 3 time-signal intensity curve within solid tissue.

### Reference standard

The reference standard was histopathologic diagnosis, following the Guidelines of the World Health Organization's International Classification of Ovarian Tumors (19).

Borderline ovarian tumors were classified as malignant disease for statistical purposes. For adnexal masses not subjected to histopathologic examination, the criteria for benign disease were based on clinical and imaging monitoring for at least 12 months, following the usual clinical care protocols of the institution.

### Statistical analysis

We analyzed data using a dedicated statistical software (R Environment for Statistical Computing software). The odds ratio (OR) and chi-squared test were used to examine associations between categorical variables. Statistical calculations were performed using 95% confidence intervals (CIs), with *P* values <0.05 considered to be statistically significant. Normally distributed data were presented as means and standard deviations (SDs).

We calculated the sensitivity, specificity, positive and negative predictive values, and area under the receiver operating characteristic (ROC) curve for ADNEX MR scores, using  $\geq 4$  as the cutoff for malignancy, as suggested by Thomassin-Naggara et al. (17). Interobserver agreement on ADNEX MR scores was evaluated using unweighted and Fleiss kappa indices.

## Results

Patients with malignant disease were older than those with benign lesions (mean age, 57.8±13.2 vs. 47.1±14.9 years). In addition, postmenopausal status predominated in patients with malignant disease compared with those with benign lesions (68.4% [54/79] vs. 37.4% [59/158]; *P* < 0.001).

Table 2 shows final diagnostic data for the 237 adnexal masses. For 164 lesions (76.7%), final diagnoses were obtained by pathologic examination of surgical or percutaneous biopsy specimens. For 73 lesions (23.3%), diagnoses were based on at least 12 months of imaging follow-up. Ovarian tumors comprised most benign and malignant masses (80%), and most were of epithelial origin. Germ cell tumors were the second most frequent lesion type in women with benign disease, followed by endometriomas and stromal/functional tumors. In women with malignant tumors, serous adenocarcinoma was the most frequent diagnosis, followed by clear cell and metastatic tumors.

Table 3 shows results for all MRI parameters evaluated. Apart from tumor size (mean value of the orthogonal mass axes),

**Table 1.** MRI scanning parameters

	Axial T1WI	Axial T2WI	Sagittal T2WI	Coronal T2WI
Fat saturation	-	Fat Sat	-	-
Timing of contrast	-	-	-	-
Sequence	Fast spin-echo	Fast-recovery Fast spin-echo	Fast-recovery Fast spin-echo	Fast-recovery Fast spin-echo
Number of dimensions	2D	2D	2D	2D
TE (ms)	12	79	115	84
TR (ms)	650	3250	3416	5166
Echo train length	4	17	26	17
Flip angle (°)	90	90	90	90
Number of averages	1	1	2	1
FOV (cm)	25–30	25–30	25–30	25–30
Slice thickness/interval (mm)	5.0/5.5	5.0/5.5	5.0/6.0	5.0/6.0
Matrix size	288×224	288×224	320×224	320×224
b value (s/mm <sup>2</sup> )	-	-	-	-
Number of phases	-	-	-	-
Approximate acquisition time	2:04	2:41	2:04	2:19
	Axial T2WI	Axial DWI	Axial T1WI	Axial T1WI contrast-enhanced
Fat saturation	-	-	Fat Sat	Fat Sat
Timing of contrast	-	-	Precontrast	Dynamic
Sequence	Fast-recovery Fast spin-echo	Echoplanar	Gradient echo	Gradient echo
Number of dimensions	2D	2D	3D	3D
TE (ms)	126	78	2072	2072
TR (ms)	3886	6975	4308	4308
Echo train length	26	1	1	1
Flip angle (°)	90	90	12	12
Number of averages	1	6	0.72	0.72
FOV (cm)	25–30	35	25–30	25–30
Slice thickness/interval (mm)	5.0/5.5	5.0/5.5	3.8/2.0	3.8/2.0
Matrix size	320×224	192×92	320×192	320×192
b value (s/mm <sup>2</sup> )	-	0, 500, 1000	-	-
Number of phases	-	-	-	5
Approximate acquisition time	2:02	4:05	0:17	2:30

T1WI, T1-weighted imaging; T2WI, T2-weighted imaging; Fat Sat, fat saturated; 2D, two dimensional; TE, echo time; TR, repetition time; FOV, field of view; DWI, diffusion-weighted imaging.

all parameters considered in scoring differed individually between malignant and benign masses. Type 3 time-signal intensity curves were associated strongly with ma-

lignant disease (35/58 malignant tumors) with respective ORs of 455 and 9.5 when compared with type 1 and 2 curves; and consistently ruled out benignity (only 1 in

20 women with benign disease presented this characteristic). Figs. 2, 3, and 4 illustrate three different types of adnexal masses and their respective enhancement curves.

**Table 2.** Final diagnosis for 237 adnexal masses

Final diagnosis	n (%)
Means of establishing diagnosis	
Imaging follow-up findings ( $\geq 1$ year)	73 masses (23.3)
Histopathologic results	164 masses (76.7)
Benign disease* (n=85)	
Ovarian	
Cystadenoma	29 (34.1)
Stromal tumor	5 (5.9)
Germ cell tumor	18 (21.2)
Endometrioma	9 (10.6)
Functional	5 (5.9)
Ovarian torsion	2 (2.3)
Non-ovarian	
Hydrosalpinx	7 (8.2)
Leiomyoma	7 (8.2)
Peritoneal or mesothelial tumor	3 (3.5)
Malignant disease* (n=79)	
Ovarian borderline	
Serous borderline	9 (11.4)
Mucinous borderline	6 (7.6)
Ovarian malignant	
Serous	24 (30.4)
Mucinous	4 (5.0)
Carcinosarcoma	3 (3.8)
Clear cell	8 (10.1)
Endometrioid	3 (3.8)
Germ cell tumor	1 (1.3)
Sex-cord stromal tumor	3 (3.8)
Metastasis	9 (11.4)
Non-ovarian	
Tubal cancer	2 (2.5)
Peritoneal cancer	5 (6.3)
Uterine cancer	1 (1.3)
Other (lymphoma)	1 (1.3)
Total of lesions	164

Data are presented as the number of lesions with rounded percentages in parentheses.

\*According to histopathologic results.

disease showed 94.9% (95% CI, 87.54%–98.60%) sensitivity and 97.5% (95% CI, 93.65%–99.31%) specificity, with accuracy of 96.62% (95% CI, 93.46%–98.53%). The positive and negative predictive values were 94.8% and 97.4%, respectively. The positive likelihood ratio was 37.5 (95% CI, 14.23–98.81) and the negative likelihood ratio was 0.05 (95% CI, 0.02–0.14). The four malignant adnexal masses that received a score of 3 (probably benign) were borderline tumors without solid tissue. The four benign adnexal masses that received a score of 4 were: one endometrioma with extensive pelvic adhesions, one broad ligament leiomyoma, and two serous cystadenomas. The level of interobserver agreement on the final classification of lesions using the ADNEX MR scoring system based on simplified MRI protocol was high ( $\kappa = 0.91$ ). The area under the ROC curve for ADNEX MR scores was 0.98 (95% CI, 0.96–0.99), demonstrating that  $\geq 4$  was the optimal cut-off point for malignancy (Fig. 5).

## Discussion

This study showed that the ADNEX MR scoring system is of great value, even based on a simplified MRI protocol, as it combines optimum MRI parameters in the evaluation of malignancy probability in women with adnexal masses. In our sample of adnexal masses, this MRI scoring system had high performance indicators, such as sensitivity and specificity values exceeding 94%. Importantly, our study corroborates the results reported by the proponents of the original ADNEX MR scoring system (17), with the use of a simple dynamic contrast-enhanced curve that can easily be obtained in clinical practice. The use of a simplified MRI protocol can catalyze the use and dissemination of ADNEX MR scoring system in the adnexal masses assessment. We also obtained a very high level of agreement between readers, which demonstrates its reproducibility.

The standardization of preoperative imaging evaluation of adnexal masses is highly desirable, as misinterpretation of results and reporting bias can lead to severe consequences for patients, most notably, unnecessary surgery and/or delayed onset of the treatment of potentially lethal disease (20). Several attempts to address failures in imaging methods are currently underway; they range from the modelling of US evaluation and reporting, such as the simple rules of the International Ovarian Tumor Analysis group (6, 7), to the proposition

Performance indicators for the ADNEX MR scoring system based on simplified MRI protocol are presented in Table 4. The originally proposed cutoff of  $\geq 4$  for malignant

**Table 3.** MRI parameters of benign and malignant masses

MRI parameters	Benign disease (n=158)	Malignant disease (n=79)	P	OR	95% CI
Size (cm)	9.11±6.5	9.16±6.5	0.33		
Septum			0.0008		
Single	25/54 (46.2)	3/35 (8.6)			
Two or more	29/54 (53.8)	32/35 (91.4)		9.2	2.50–33.69
Septum thickness			<0.0001		
Thin	37/54 (68.5)	2/35 (5.8)			
Thick	17/54 (31.5)	33/35 (94.2)		26.2	5.55–123.58
T2-weighted signal intensity within solid tissue			<0.001		
Low	17/23 (74.0)	2/70 (2.8)			
Medium/high	6/23 (26)	68/70 (97.2)		96.3	17.84–520.13
b=1000 s/mm <sup>2</sup> -weighted signal intensity within solid tissue			<0.0001		
Low	17/25 (68)	2/69 (2.9)			
Medium/high	8/25 (32)	67/69 (97.1)		72.25	14.04–371.76
Wall enhancement			<0.0001		
No	45/100 (45.0)	0			
Yes	55/100 (55.0)	42/42 (100)		69.68	4.17–1163.88
Time-signal intensity curve within solid tissue			<0.0001		
Type 1	13/20 (65)	1/58 (1.7)			
Type 2	6/20 (30.0)	22/58 (38)			
Type 3	1/20 (5.0)	35/58 (60.3)			
Type 3 vs. type 1			<0.0001	455	26.47–7819.06
Type 3 vs. type 2			0.042	9.5	1.07–84.71
Type 2 vs. type 1			0.0007	47.66	5.14–441.21
Ascites			<0.0001		
No	134/158 (84.8)	26/79 (45.6)			
Yes	24/158 (15.2)	43/79 (54.4)		9.2	4.80–17.73
Peritoneal implants			0.0001		
No	158/158 (100)	40/79 (50.7)			
Yes	0	39/79 (49.3)		309.17	18.6–5138.48
Metastasis			0.02		
No	158/158 (100)	73/79 (92.7)			
Yes	0	6/79 (7.6)		28.03	1.55–504.30

Data are expressed as mean ± standard deviation or n/N (%). The denominators used to calculate percentages varied according to the availability of data. MRI, magnetic resonance imaging; OR, odds ratio; CI, confidence interval.

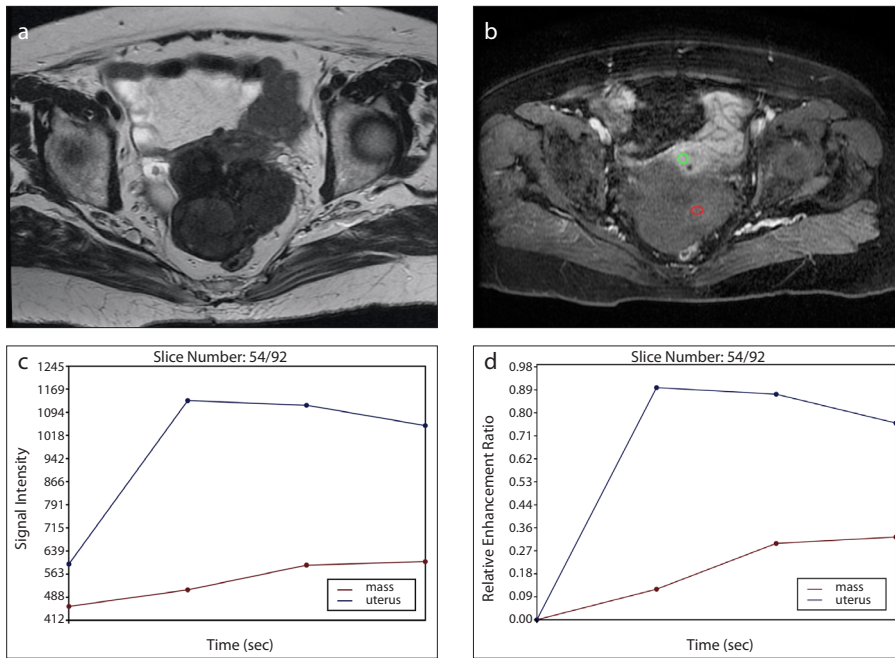


**Figure 2. a–d.** Right adnexal mass with irregular contour, undetermined by IOTA simple rules in a 74-year-old woman. Final ADNEX MR score of 2. Follow-up since 2015 shows stability of the findings. Axial T2-weighted spin-echo image (a) shows a well-defined, lobulated low signal intensity solid tumor. Axial contrast-enhanced study (b) demonstrates low level of enhancement of the mass (green circle ROI, uterus; red circle ROI, adnexal mass). Signal intensity curve (c) shows gradual increase in the signal intensity of the solid tissue on the dynamic contrast-enhanced images, without a peak (type 1 curve). Relative enhancement ratio (d) shows gradual increase in mass enhancement compared with the uterus, without a peak (type 1 curve).

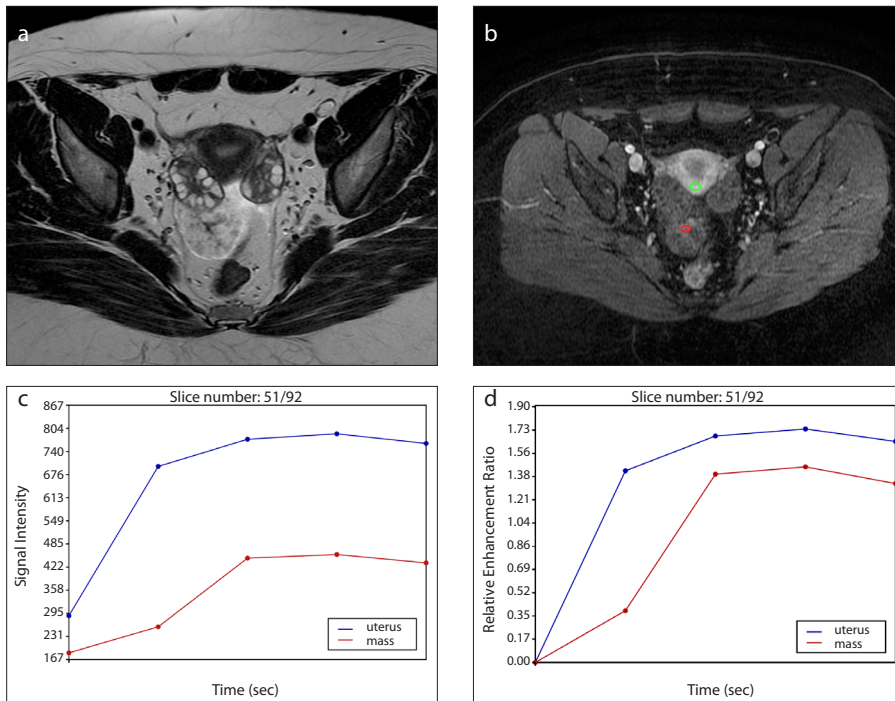


**Figure 3. a–d.** Pelvic mass of undefined etiology in a 23-year-old woman. Final ADNEX MR score of 4. Right salpingo-oophorectomy plus omentectomy was performed; a borderline serous tumor of right ovary was the histologic diagnosis. Axial T2-weighted spin-echo image (a) demonstrates a cystic mass with solid components adhered to the right ovary. Axial contrast-enhanced study demonstrates inhomogeneous enhancement of the mass (green circle ROI, uterus; red circle ROI, adnexal mass). Signal intensity curve (c) shows moderate initial increase in the signal intensity of solid tissue, followed with a plateau (type 2 curve). Relative enhancement ratio (d) shows moderate initial increase in mass enhancement compared with the uterus, followed by a plateau.

of MRI evaluation algorithms (11, 15). Our study strengthens a new MRI reporting system for assessing the risk of malignancy of adnexal masses, tested in a large set of patients with complete clinical and pathologic data. Even with the use of the simplified contrast-enhanced dynamic protocol, we obtained adequate enhancement curves, enabling use of the protocol in diagnostic centers lacking MRI magnets and/or software and technology for the acquisition and postprocessing of advanced dynamic contrast-enhanced sequences. The total MRI acquisition time was good, a little more than 18 minutes, using the current protocol. Another practical technical point learned is that diffusion-weighted images with b value of 500 s/mm<sup>2</sup> are unnecessary and useless, being recommended to use only with b values of 0 and 1000 s/mm<sup>2</sup>, which could reduce the total time by 99 s.

The standardization of reporting (i.e., with systems such as BI-RADS™, PI-RADS™, and LI-RADS™) improves communication between radiologists and clinicians and reduces misunderstanding. In clinical use, the objective of the ADNEX MR scoring system is that scores ≥4 indicate the need for prompt surgery in a tertiary center, whereas scores of 2 and 3 suggest a higher probability of benignity, indicating follow-up or minimally invasive surgery. Although MRI is considerably more expensive than US, it plays an important role in the preoperative discrimination of indeterminate adnexal masses found on US. Risk stratification with ADNEX MR scoring system could improve overall cost optimization, as unnecessary surgery can be avoided in low-risk patients (with scores ≤3), and high-risk patients (with scores ≥4) can be referred for urgent laparotomy in specialized oncologic centers (12, 21). Four borderline tumors (cystic masses without solid tissue) were assigned a score of 3, reflecting some difficulty with the use of the system. However, no invasive malignant tumor received a score <4, showing that the method may rarely lead to unnecessary surgery. More detailed cost-benefit studies are needed to verify the real impact of the system's application on cost optimization and possibly gain in time.

Our study has some limitations. First, it was conducted in a tertiary oncology center, with a high prevalence of malignant or suspicious adnexal lesions. Second, the participating radiologists had different expertise and backgrounds relevant to the MRI

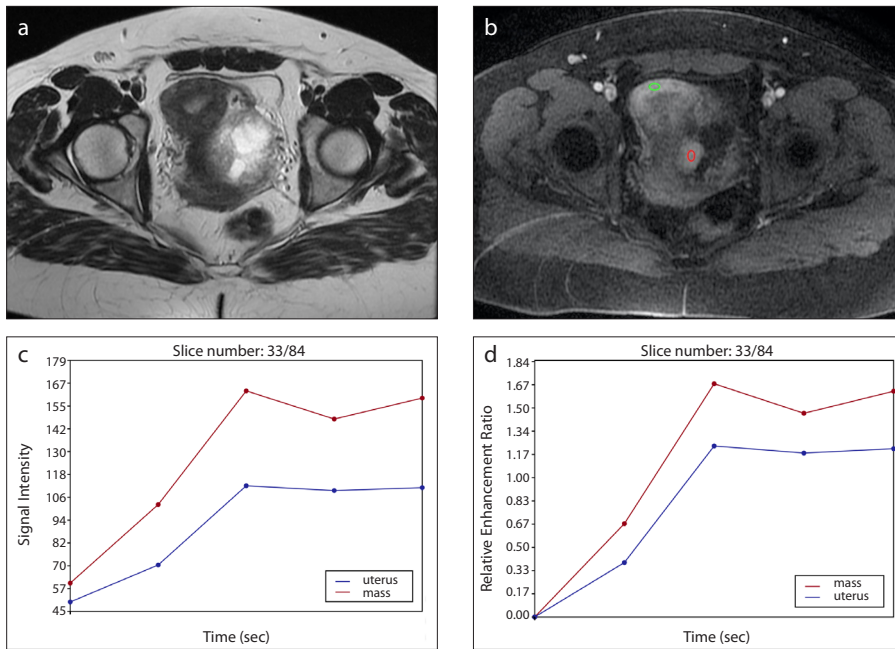


**Figure 4. a–d.** Pelvic mass of undefined etiology on ultrasound examination in a premenopausal 41-year-old woman. Final ADNEX MR score of 5. Postsurgical histologic diagnosis was Sertoli-Leydig malignant tumor. Axial T2-weighted spin-echo image (a) demonstrates cystic mass with solid components in the left para-uterine region. Venous supply of the mass was through the left ovarian vein (not shown). Axial contrast-enhanced study demonstrates enhancement of the solid component (green circle ROI, uterus; red circle ROI, adnexal mass). Signal intensity curve (c) shows an initial increase in the signal intensity of solid tissue that was steeper than that of myometrium (type 3 curve). Relative enhancement ratio (d) shows intense initial increase in mass enhancement compared with the uterus.

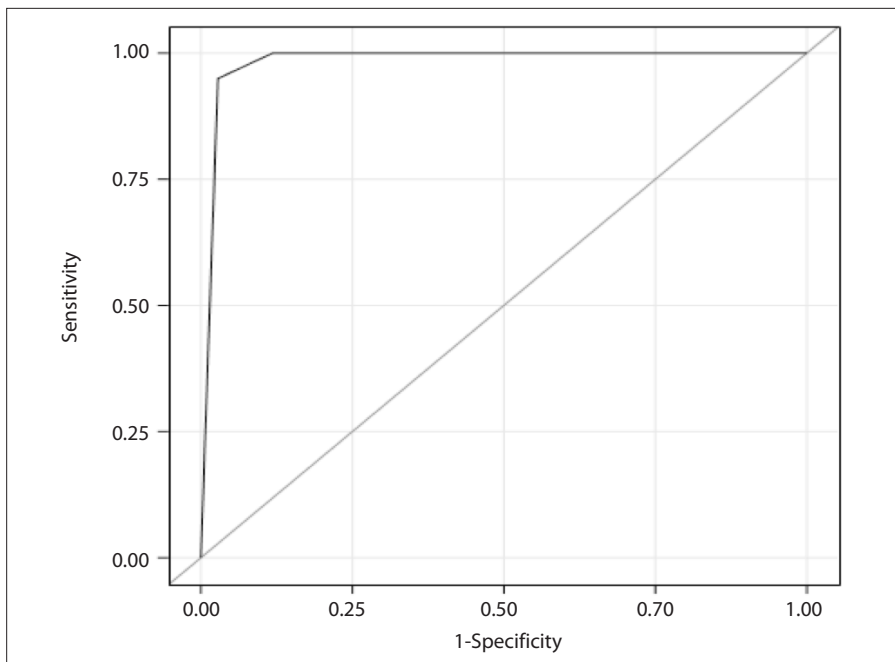


**Figure 5.** The area under the curve (AUC) of the ADNEX MR score using scores > 4 as the cutoff for malignant disease, as suggested by Thomassin-Naggara et al. (17). AUC was 0.98 (95%CI, 0.96–0.99).

evaluation of adnexal masses. However, both professionals were relatively seasoned radiologists with  $\geq 6$  years of professional activity. The inclusion of medical residents

(inexperienced readers) in a further evaluation of score reproducibility would be desirable. Third, the sample included a limited number of borderline ovarian tumors,

**Table 4.** Final ADNEX MR score for all 237 adnexal masses

ADNEX MR score	Benign disease	Malignant disease
Score 1	4 (2.5)	0
Score 2	123 (77.9)	0
Score 3	27 (17.1)	4 (5.1)
Score 4	4 (2.5)	21 (26.6)
Score 5	0 (0)	54 (68.3)
Total	158 (100)	79 (100)

Data are presented as n (%).

whose evaluation is most challenging. Fourth, we considered patients who were not operated, but were followed for at least 1 year with no sign of disease, to be “negative”; this interval may be short for some ovarian diseases, such as borderline tumors, which can evolve slowly.

In conclusion, at a tertiary cancer center, the ADNEX MR scoring system, even based on a simplified MRI protocol, was of great value in the standardization of MRI evaluation and reporting for adnexal masses. The system showed excellent performance in our institution, as it did in the original study. The next step is to test and refine the scoring system for application to masses that are difficult to evaluate using US and to further improve the parameters, enabling better identification of borderline ovarian tumors (e.g., with the use of the simplified system in combination with other imaging or laboratory methods).

#### Conflict of interest disclosure

The authors declared no conflicts of interest.

#### References

- Pickhardt PJ, Hanson ME. Incidental adnexal masses detected at low-dose unenhanced CT in asymptomatic women age 50 and older: implications for clinical management and ovarian cancer screening. *Radiology* 2010; 257:144–150. [CrossRef]
- Menon U, Griffin M, Gentry-Maharaj A. Ovarian cancer screening—current status, future directions. *Gynecol Oncol* 2014; 132:490–495. [CrossRef]
- Forstner R, Sala E, Kinkel K, Spencer JA. ESUR guidelines: ovarian cancer staging and follow-up. *Eur Radiol* 2010; 20:2773–2780. [CrossRef]
- Webb PM, Jordan SJ. Epidemiology of epithelial ovarian cancer. *Best Pract Res Clin Obstet Gynaecol* 2017; 41:3–14. [CrossRef]
- Coccia ME, Rizzello F, Romanelli C, Capezzuoli T. Adnexal masses: what is the role of ultrasonographic imaging? *Arch Gynecol Obstet* 2014; 290:843–854. [CrossRef]

6. Timmerman D, Valentin L, Bourne TH, Collins WP, Verrelst H, Vergote I. Terms, definitions and measurements to describe the sonographic features of adnexal tumors: a consensus opinion from the International Ovarian Tumor Analysis (IOTA) Group. *Ultrasound Obstet Gynecol* 2000; 16:500–505. [\[CrossRef\]](#)
7. Timmerman D, Ameye L, Fischerova D, et al. Simple ultrasound rules to distinguish between benign and malignant adnexal masses before surgery: prospective validation by IOTA group. *BMJ* 2010; 341:c6839–c6839. [\[CrossRef\]](#)
8. Timmerman D, Van Calster B, Testa A, et al. Predicting the risk of malignancy in adnexal masses based on the Simple Rules from the International Ovarian Tumor Analysis group. *Am J Obstet Gynecol* 2016; 214:424–437. [\[CrossRef\]](#)
9. Kaijser J, Vandecaveye V, Deroose CM, et al. Imaging techniques for the pre-surgical diagnosis of adnexal tumours. *Best Pract Res Clin Obstet Gynaecol* 2014; 28:683–695. [\[CrossRef\]](#)
10. Sohaib SA, Mills TD, Sahdev A, et al. The role of magnetic resonance imaging and ultrasound in patients with adnexal masses. *Clin Radiol* 2005; 60:340–348. [\[CrossRef\]](#)
11. Spencer JA, Ghattamaneni S. MR imaging of the sonographically indeterminate adnexal mass. *Radiology* 2010; 256:677–694. [\[CrossRef\]](#)
12. Rieber A, Nüssle K, Stöhr I, et al. Preoperative diagnosis of ovarian tumors with MR imaging. *AJR Am J Roentgenol* 2001; 177:123–129. [\[CrossRef\]](#)
13. Anthonakakis C, Nikoloudis N. Pelvic MRI as the “gold standard” in the subsequent evaluation of ultrasound-indeterminate adnexal lesions: a systematic review. *Gynecol Oncol* 2014; 132:661–668. [\[CrossRef\]](#)
14. Dodge JE, Covens AL, Lacchetti C, et al. Preoperative identification of a suspicious adnexal mass: a systematic review and meta-analysis. *Gynecol Oncol* 2012; 126:157–166. [\[CrossRef\]](#)
15. Forstner R, Thomassin-Naggara I, Cunha TM, et al. ESUR recommendations for MR imaging of the sonographically indeterminate adnexal mass: an update. *Eur Radiol* 2017; 27:2248–2257. [\[CrossRef\]](#)
16. Allen BC, Hosseinzadeh K, Qasem SA, Varner A, Leyendecker JR. Practical approach to MRI of female pelvic masses. *AJR Am J Roentgenol* 2014; 202:1366–1375. [\[CrossRef\]](#)
17. Thomassin-Naggara I, Aubert E, Rockall A, et al. Adnexal masses: development and preliminary validation of an MR imaging scoring system. *Radiology* 2013; 267:432–443. [\[CrossRef\]](#)
18. Sadowski EA, Robbins JB, Rockall AG, Thomassin-Naggara I. A systematic approach to adnexal masses discovered on ultrasound: the AD-NEEx MR scoring system. *Abdom Radiol* 2017; 1–17.
19. Kurman RJ, Carcangiu ML, Herrington CS YR. World Health Organization Classification of Tumours of Female Reproductive Organs. 4th ed. International Agency for Research on Cancer; 2014.
20. Ratner ES, Staib LH, Cross SN, Raji R, Schwartz PE, McCarthy SM. The clinical impact of gynecologic MRI. *AJR Am J Roentgenol* 2015; 204:674–680. [\[CrossRef\]](#)
21. Medeiros LR, Freitas LB, Rosa DD, et al. Accuracy of magnetic resonance imaging in ovarian tumor: a systematic quantitative review. *Am J Obstet Gynecol* 2011; 204:67.e1–e10. [\[CrossRef\]](#)